RESEARCH ARTICLE | AUGUST 18 2010

High sensing properties of magnetic plasmon resonance in the double-rod and tri-rod structures

J. X. Cao; H. Liu; T. Li; S. M. Wang; Z. G. Dong; S. N. Zhu

Appl. Phys. Lett. 97, 071905 (2010)
https://doi.org/10.1063/1.3481359

High sensing properties of magnetic plasmon resonance in the double-rod and tri-rod structures

J. X. Cao,[1] H. Liu,[1,a)] T. Li,[1] S. M. Wang,[1] Z. G. Dong,[2] and S. N. Zhu[1,a)]
[1]*National Laboratory of Solid State Microstructures, Nanjing University, Nanjing 210093, China*
[2]*Department of Physics, Southeast University, Nanjing 211189, People's Republic of China*

(Received 12 June 2010; accepted 28 July 2010; published online 18 August 2010)

We numerically investigated the magnetic plasmon resonances in the double-rod and tri-rod structures (DRSs and TRSs) for sensing applications. Like localized surface plasmon modes in nanostructures, the magnetic plasmon resonance wavelengths are sensitive to refractive index changes in the environment medium. The electromagnetic fields near DRSs and TRSs were much more localized in the dielectric surrounding the structures at the resonance wavelengths, which caused the linewidth of magnetic responses narrower. A large figure of merit could be obtained in the magnetic plasmon modes of DRSs and TRSs, which enables the use of the structures as sensing elements with remarkable performance. © *2010 American Institute of Physics*.
[doi:10.1063/1.3481359]

Optical sensors based on the excitation of surface plasmon resonance in nano-metallic structures have been greatly developed in recent years due to their great local field enhancement effect.[1–8] Various shapes of metal nanoparticle have been proposed, such as nanorods,[9] nanoshells,[10] nanocages,[11] and nanostars.[12] Simultaneously, refractive index sensing through quasi-one-dimensional nanoslit structures for large area has been reported.[13] Recently, Marek Piliarik *et al.* predicted the ultimate performance of all major configurations of surface plasmon resonance sensors.[14] DRSs were proposed by Shalaev *et al.* to realize magnetic plasmon resonance and negative refraction in infrared frequency ranges.[15] In our previous work, TRSs were reported and could be seen as two coupled DRSs. Due to the strong hybridization effect in TRSs, omnidirectional negative refraction[16] and great polarization changes[17] were realized.

In this article, the magnetic plasmon modes in DRSs and TRSs were employed to realize high-quality sensing. The provided structures could be fabricated through electrochemical anodization method in.[18] We investigated the sensing properties of the magnetic plasmon modes in DRSs and TRSs and compared them with those of the localized surface plasmon modes in SRSs. Based on the simulations, the electromagnetic fields were greatly confined to the dielectric surrounding the designed structures at the magnetic plasmon resonance wavelengths, indicating the narrow linewidth of magnetic responses. Simultaneously, the magnetic plasmon modes were sensitive to refractive index changes in the surrounding dielectric. Together with the sharp dip and narrow full-width at half-maximum (FWHM) of the transmission curves, the magnetic plasmon modes of DRSs and TRSs showed sensing performance far superior to that of the electric plasmon modes in SRSs. In particular, the short wavelength hybrid mode in TRSs showed a figure of merit (FOM) of 88.3, larger than that of other investigated structures here.

Figures 1(a) and 1(b) represent the schematic of the unit cell for DRSs and TRSs. Both two cube unit cells had the same length of side $p=500$ nm. The length and cross-section diameter of the gold rods were $h=300$ nm and $d=100$ nm, respectively. The gap between the rods was $g=20$ nm. The boundary of the cells in the x- and y-direction was defined as a periodic condition; that in the z-direction was set as an open condition. We first set the medium surrounding the gold rods as air ($n=1$) and studied the magnetic responses and transverse electric field distributions. Afterwards, we changed the refractive index of the surrounding medium to investigate the enhanced sensing characteristics.

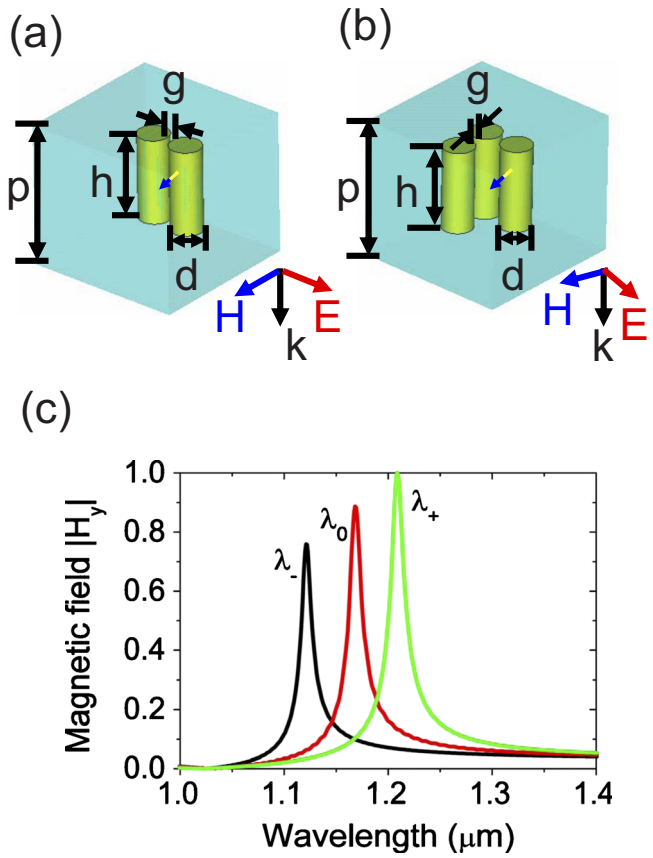

FIG. 1. (Color online) Schematics of unit cell for (a) DRSs and (b) TRSs. (c) Normalized magnetic field amplitude $|H_y|$ detected by the probes shown in Figs. 1(a) and 1(b).

a)Authors to whom correspondence should be addressed. Electronic addresses: liuhui@nju.edu.cn and zhusn@nju.edu.cn.

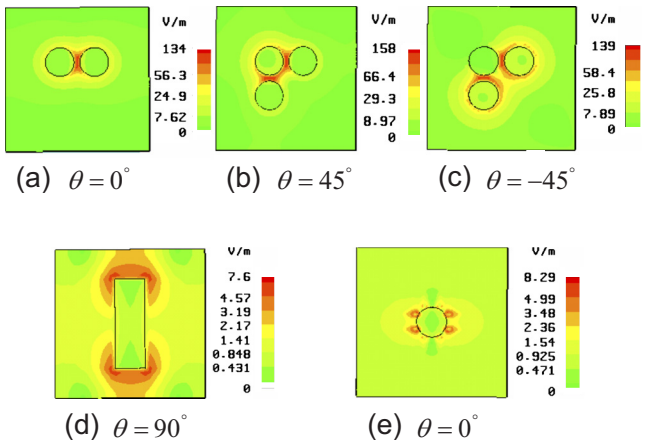

FIG. 2. (Color online) Electric field patterns at resonance wavelengths(a) λ_0 for DRSs, (b) λ_+ and (c) λ_- for TRSs, (d) LLSP, and (e) TLSP wavelengths for SRSs. The angle θ in the figures showed the directions of the incident electric fields.

To study the magnetic plasmon characters of the proposed structures, a commercial software package CST MICROWAVE STUDIO (Computer Simulation Technology GmbH, Darmstadt, Germany) was employed in the numerical analysis. The permittivity of gold was satisfied with the Drude model: $\varepsilon(\omega)=1-\omega_p^2/(\omega^2+i\omega_\tau\omega)$ with the plasma frequency $\omega_p=2\pi\times2.175\times10^{15}$ s^{-1} and the damping constant $\omega_\tau=2\pi\times6.5\times10^{12}$ s^{-1}.[19] Considering the grain boundary effect, surface scattering, and inhomogeneous broadening in the thin film, the damp constant used in the calculations was about three times large as that in bulk gold.[7]

In the simulations, the propagation direction of the linearly polarized incident wave was along the z-axis. The polarization direction was defined by the angle θ between the electric field and the x-axis. For DRSs, the magnetic resonance mode was excited by the incident wave with $\theta=0°$. According to our previous work,[17] two hybrid magnetic plasmon modes could be established for TRSs. When $\theta=45°$, only the long wavelength mode (LW mode) was excited at λ_+; when $\theta=-45°$, only the short wavelength mode (SW mode) was excited at λ_-. In this article, the magnetic response of TRSs is excited by the incident waves with $\theta=45°$ and $-45°$ respectively. Figure 1(c) shows the local magnetic amplitude $|H_y|$ recorded by the probes in the gaps between the nanorods shown in Figs. 1(a) and 1(b). The resonance wavelength for DRSs was observed at $\lambda_0=1.167$ μm; while for TRSs, the resonance wavelengths were at $\lambda_+=1.208$ μm and $\lambda_-=1.121$ μm. To study the resonance properties of the three magnetic plasmon modes, the Q factors of DRSs and TRSs were calculated based on the definition $Q=2\pi\lambda/\Delta\lambda$, where λ and $\Delta\lambda$ were the resonance wavelengths and FWHM of the resonance peak. From our simulation results, the calculated Q factor of the magnetic plasmon mode in DRSs was $Q_0=806.87$. For LW and SW modes in TRSs, the Q factors were $Q_+=764.99$ and $Q_-=934.21$. Obviously, the Q factor of SW mode in TRSs was the best.

Figures 2(a)–2(c) show the electric field patterns in the end plane ($z=300$ nm) of the nanorods at λ_0 for DRSs, and λ_+ and λ_- for TRSs, respectively. For DRSs, the electric field was localized around the rods, especially in the gap of the two nanorods as shown in Fig. 2(a). For TRSs, the two induced currents oscillated along the same direction in the middle rod for LW mode but in the opposite directions for SW mode.[17] As a result, the electric field circled the middle-rod at λ_+ shown in Fig. 2(b) and circled the two side-rods at λ_- shown in Fig. 2(c). In order to provide good comparison, the plasmon resonance of SRS with the same periodicity and boundary conditions was also investigated. Two different plasmon modes could be excited in SRS under different incident polarization directions. The longitudinal mode (LLSP mode) was excited by the electric field along the rod shown in Fig. 2(d); the transverse mode (TLSP mode) was excited by the electric field perpendicular to the rod shown in Fig. 2(e). The comparison of Fig. 2 showed that the property of localization field in DRSs and TRSs was better than that in SRSs.

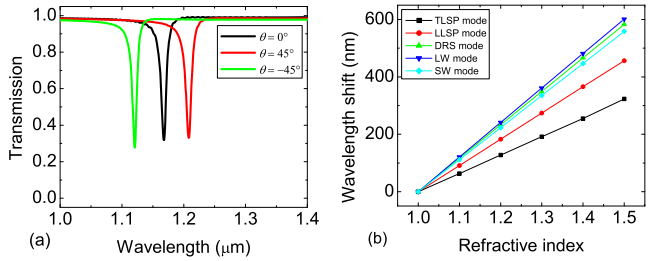

FIG. 3. (Color online) (a) Transmissions of metamaterials based on DRSs and TRSs with the refractive index of the background $n=1$. (b) Dependence of resonant wavelength shifts on the refractive index of the background in DRSs and TRSs, together with that in SRSs.

Like surface plasmon resonance, magnetic plasmon modes were also very sensitive to the refractive index change in the surrounding materials. Simultaneously, the linewidth of magnetic response was narrow due to better property of localizing field and lower radiation loss.[20,21] Thus, DRSs and TRSs could be used as highly sensitive sensors. Figure 3(a) shows the transmission curves of DRSs and TRSs with the refractive index of the background $n=1$ for the above incident cases. The sharp dips in the figure indicated the three magnetic plasmon modes. According to the simulations, when the refractive index of the surrounding dielectric varied from 1.0 to 1.4, the resonance wavelength of DRSs shifted from 1.167 to 1.634 μm. For TRSs, the resonance wavelength shifted from 1.208 to 1.689 μm for LW mode and from 1.121 to 1.567 μm for SW mode. The dependence of magnetic resonant wavelength shifts to the refractive index of the surrounding dielectric in DRSs and TRSs were represented in Fig. 3(b). It can be seen that the resonance wavelength shifts of the magnetic plasmon modes were perfectly linear over the whole refractive index range. The sensitivity, denoted as the slope of the resonance wavelength over the refractive index change, was 1175.9 nm/refractive index unit (*RIU*) for the magnetic plasmon mode of DRSs. For LW mode of TRSs, the sensitivity was 1194.6 nm/RIU and larger than that of DRSs. For SW mode, the sensitivity was 1114.3 nm/RIU and smaller than that of DRSs. To demonstrate the advantage of the magnetic plasmon modes for sensing, we also calculated the sensitivity of the electric plasmon resonances of SRSs. The sensitivity was 912.7 nm/RIU for LLSP mode and 633.8 nm/RIU for TLSP mode, both of which were much smaller than those of the magnetic plasmon modes of DRSs and TRSs.

To directly compare the overall sensing performance of the electric plasmon modes in SRSs and the magnetic plas-

TABLE I. Calculations of sensing performance by figure of merit (FOM) for the plasmon modes, together with the corresponding sensitivity m.

Eigenmode	m(nm/RIU)	FOM
LLSP mode	912.7	2.55
TLSP mode	633.8	30.2
MPR of DRS	1175.9	74.6
LW mode	1194.6	69.2
SW mode	1114.3	88.3

mon modes in DRSs and TRSs, a useful concept of FOM was used defined as follows:[1,6]

$$\mathrm{FOM} = \frac{m(\mathrm{nm/RIU})}{\mathrm{FWHM(nm)}}(1 - T_{\min}), \tag{1}$$

where m is the slope of the resonance wavelength shift over the refractive index change. The calculated values m and FOM were given in Table I. It could be seen that the magnetic plasmon modes showed better sensing performance than the electric plasmon modes due to the high sensitivity and narrow linewidth of transmission curves. For instance, the FOM for SW mode was 88.3, approximately 18.4% greater than that of the magnetic plasmon mode in DRSs and more than 33 times as that of LLSP mode in SRSs. According to the above analysis, SW mode had a higher quality factor. Thus, the best FOM could still be obtained in SW mode even though its sensitivity was a little smaller. The dependence of the FOM for the magnetic plasmon modes in DRSs and TRSs on the structural parameter diameter, length and gap of the nanorods were shown in Figs. 4(a)–4(c), respectively. It could be found that the bigger diameter, shorter length, and smaller gap indicated better sensing performance. In fact, when the length of the nanorod is too short, the scattering loss due to microfabrication and the Ohmic loss of metal component will prevent higher sensing performance.

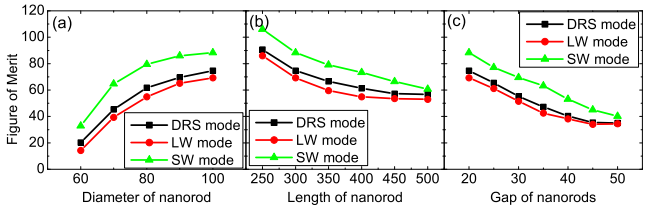

FIG. 4. (Color online) FOM for sensing properties of magnetic plasmon modes in DRSs and TRSs depending on the structure parameters of (a) diameter, (b) length, and (c) gap of nanorods, respectively.

In conclusion, we numerically investigated the sensing properties of the magnetic plasmon modes of DRSs and TRSs. The electromagnetic field was strongly confined within the proposed structures at the magnetic plasmon modes, leading to greater field-material interactions and the narrow linewidth of the magnetic responses. Together with the sensitivity of the magnetic plasmon modes to the refractive index changes of the surrounding medium, the transmission for the excitation of the hybrid SW mode of TRSs possessed a good FOM of 88.3. Compared with the electric plasmon modes in SRSs, the magnetic plasmon modes had higher sensitivity and could offer better performance as sensors in the infrared range.

This work was supported by the National Natural Science Foundation of China (Grants Nos. 10704036, 10874081, 60907009, 10904012, 10974090, and 60990320) and by the National Key Projects for Basic Research of China (Grants Nos. 2006CB921804, 2009CB930501, and 2010CB630703).

[1] L. J. Sherry, S. H. Chang, G. C. Schatz, R. P. Van Duyne, B. J. Wiley, and Y. N. Xia, Nano Lett. **5**, 2034 (2005).
[2] H. W. Liao, C. L. Nehl, and J. H. Hafner, Nanomedicine **1**, 201 (2006).
[3] H. Wang, D. W. Brandl, F. Le, P. Nordlander, and N. J. Halas, Nano Lett. **6**, 827 (2006).
[4] J. N. Anker, W. P. Hall, O. Lyandres, N. C. Shah, J. Zhao, and R. P. Van Duyne, Nature Mater. **7**, 442 (2008).
[5] J. Homola, Chem. Rev. **108**, 462 (2008).
[6] K. M. Byun, S. J. Kim, and D. Kim, Appl. Opt. **46**, 5703 (2007).
[7] N. Liu, L. Langguth, T. Weiss, J. Kästel, M. Fleischhauer, T. Pfau, and H. Giessen, Nature Mater. **8**, 758 (2009).
[8] A. Artar, A. A. Yanik, and H. Altug, Appl. Phys. Lett. **95**, 051105 (2009).
[9] H. Wang, T. B. Huff, D. A. Zweifel, W. He, P. S. Low, A. Wei, and J. Cheng, Proc. Natl. Acad. Sci. U.S.A. **102**, 15752 (2005).
[10] S. J. Oldenburg, R. D. Averitt, S. L. Westcott, and N. J. Halas, Chem. Phys. Lett. **288**, 243 (1998).
[11] J. Y. Chen, F. Saeki, B. J. Wiley, H. Cang, M. J. Cobb, Z. Y. Li, L. Au, H. Zhang, M. B. Kimmey, X. D. Li, and Y. N. Xia, Nano Lett. **5**, 473 (2005).
[12] C. L. Nehl, H. W. Liao, and J. H. Hafner, Nano Lett. **6**, 683 (2006).
[13] M. Hyung, H. Gao, and T. W. Odom, Nano Lett. **9**, 2584 (2009).
[14] M. Piliarik and J. Homola, Opt. Express **17**, 16505 (2009).
[15] V. M. Shalaev, W. S. Cai, U. K. Chettiar, H. K. Yuan, A. K. Sarychev, V. P. Drachev, and A. V. Kildishev, Opt. Lett. **30**, 3356 (2005).
[16] F. M. Wang, H. Liu, T. Li, S. N. Zhu, and X. Zhang, Phys. Rev. B **76**, 075110 (2007).
[17] J. X. Cao, H. Liu, T. Li, S. M. Wang, T. Q. Li, S. N. Zhu, and X. Zhang, J. Opt. Soc. Am. B **26**, B96 (2009).
[18] J. Yao, Z. Liu, Y. Liu, Y. Wang, C. Sun, G. Bartal, A. M. Stacy, and X. Zhang, Science **321**, 930 (2008).
[19] M. A. Ordal, L. L. Long, R. J. Bell, S. E. Bell, R. R. Bell, R. W. Alexander, Jr., and C. A. Ward, Appl. Opt. **22**, 1099 (1983).
[20] J. D. Jackson, *Classical Electrodynamics* (Wiley, New York, 1999).
[21] H. Liu, D. A. Genov, D. M. Wu, Y. M. Liu, J. M. Steele, C. Sun, S. N. Zhu, and X. Zhang, Phys. Rev. Lett. **97**, 243902 (2006).